DOI: https://doi.org/10.14311/TPFM.2025.034

ON FLUTTER ANALYSIS BY THE FINITE ELEMENT METHOD USING TAYLOR-HOOD AND SCOTT-VOGELIUS ELEMENTS

K. Vacek [1,2], P. Sváček [2]

[1] **Institute of Mathematics of the Czech Academy of Sciences, Žitná 25, Prague 1**

[2] **Czech Technical University Department of Technical Mathematics, Karlovo náměstí 13, 121 35 Praha 2**

Abstract

This paper presents a numerical study of a complete fluid-structure interaction (FSI) problem of incompressible fluid flow interacting with a flexible supported airfoil whose motion is described by two degrees of freedom. The governing equations for the fluid flow are formulated in the arbitrary Lagrangian-Eulerian (ALE) framework and coupled to a system of ordinary differential equations describing the airfoil motion. The numerical solution is obtained using the finite element method (FEM), where both the Taylor-Hood (TH) and Scott-Vogelius (SV) elements are used. Stabilization techniques, including the streamline upwind Petrov-Galerkin (SUPG) method and grad-div stabilization, are applied to treat convection dominance and numerical oscillations. The results are validated against theoretical benchmarks, confirming the robustness and accuracy of the presented methods.

Keywords: finite element method, arbitrary Lagrangian-Eulerian method, Scott-Vogelius element, Taylor-Hood element.

1 Introduction

The study of fluid-structure interaction (FSI) plays a significant role in many engineering and scientific applications, such as the design of light aircraft drones, or other subsonic blade machines. In particular, the interaction between incompressible fluid flow and rigid structures requires a robust mathematical and numerical framework to capture all the physical phenomena, see [1, 2].

This paper addresses the problem of an interaction between an airfoil with an incompressible fluid flow. The fluid is governed by the incompressible Navier-Stokes equations, while the airfoil's motion is modeled as a rigid body with two degrees of freedom: vertical (bending) and angular (pitching) displacements. To effectively handle the moving domain, the arbitrary Lagrangian-Eulerian (ALE) framework is used, see [3, 4].

The numerical solution of the governing equations is performed using a finite element method (FEM). To guarantee the stability of the scheme, it is necessary to use the velocity pressure pair which satisfies the Babuška-Brezzi (BB) inf-sup condition, see [5]. In this paper, two such elements are considered: the Taylor-Hood (TH) and the Scott-Vogelius (SV) elements, see [5]. The first one provides a stable approximation of velocity and pressure but satisfies the divergence constraint only discretely. To improve this, the second element is employed, which strongly guarantees the divergence constraint. On the other hand, the mesh has to be created as a barycentric refinement of a regular triangulation, to guarantee BB stability, see [5].

The main application includes the convection-dominated problem, hence the stabilization methods must be applied, including the streamline upwind Petrov-Galerkin (SUPG) method for the TH element and classical streamline diffusion for the SV element, see [6]. Furthermore, grad-div stabilization is employed to mitigate nonphysical oscillations in the discretization with the TH element, see [7].

The purpose of this work is to compare the performance of these two elements in the context of an FSI problem that is the flow around the NACA0012 airfoil with two degrees of freedom. The two discretization techniques are compared with each other and with aero-elastic theory or with the nastran predictions, see [8, 9].

2 Governing equations

This section presents the mathematical formulation of the fluid-structure interaction (FSI) problem. The fluid flow is governed by the incompressible Navier-Stokes equations, which consist of the momentum and continuity equations. The moving domain is treated by the arbitrary Lagrangian-Eulerian (ALE) framework. The flow problem is equipped with appropriate initial and boundary conditions. The airfoil vibrations are described by a system of ordinary differential equations.

2.1 Incompressible fluid flow model

Let us assume a bounded computational fluid domain $\Omega_t \subset \mathbb{R}^2$ with a continuous Lipschitz boundary $\partial\Omega_t$ for every $t \in [0, T)$. The boundary $\partial\Omega_t$ consists of three separate parts $\partial\Omega_t = \Gamma_D \cup \Gamma_O \cup \Gamma_{W_t}$, where Γ_D denotes the inlet, Γ_O represents the outlet, and Γ_{W_t} is the surface of the airfoil.

In order to discretize the flow problem on a moving domain, the ALE method is employed. The ALE approach is based on the ALE transformation A_t, defined by

$$A_t : \Omega_0 \to \Omega_t, \quad X \mapsto x(X,t) = A_t(X), \quad X \in \Omega_0,\ t \in (0,T). \tag{1}$$

The ALE transformation is an extension of the mapping which projects the reference position of the interface Γ_{W_0} on the structural position Γ_{W_t} (here the subscript 0 means the position in the reference domain Ω_0) for a detailed description, see, e.g., [4].

The incompressible Navier-Stokes equations in the ALE formulation reads: we seek the pair of velocity $\boldsymbol{u}(x,t) : \Omega_t \to \mathbb{R}^2$ and the kinematic pressure $p(x,t) : \Omega_t \to \mathbb{R}$ which for any $t \in (0,T)$ in Ω_t satisfy

$$\begin{aligned} \frac{D^A}{Dt}\boldsymbol{u} + [(\boldsymbol{u}-\boldsymbol{w})\cdot\boldsymbol{\nabla}]\boldsymbol{u} - \nu\boldsymbol{\Delta}\boldsymbol{u} + \boldsymbol{\nabla} p = &\ 0, \\ \boldsymbol{\nabla}\cdot\boldsymbol{u} = &\ 0, \end{aligned} \tag{2}$$

where ν denotes the kinematic viscosity, $\frac{D^A}{Dt}$ represents the ALE derivative, and $\boldsymbol{w} = \partial A^t/\partial t$ means the domain velocity, see [2]. The problem (2) is fulfilled by the initial condition

$$\boldsymbol{u}(x,0) = \boldsymbol{u}_0 \quad \text{in } \Omega_0, \tag{3}$$

and by the boundary conditions

$$\begin{aligned} \boldsymbol{u}(x,t) = &\ \boldsymbol{g}(x,t) && \text{on } \Gamma_D \times (0,T], && \text{(4a)} \\ \boldsymbol{u}(x,t) = &\ \boldsymbol{w}(x,t) && \text{on } \Gamma_{W_t},\ t \in (0,T], && \text{(4b)} \\ -(p - p_{ref})\boldsymbol{n} + \nu\frac{\partial \boldsymbol{u}}{\partial \boldsymbol{n}} = &\ 0 && \text{on } \Gamma_O \times (0,T], && \text{(4c)} \end{aligned}$$

where $\boldsymbol{n}$ is the unit outward normal vector to $\partial\Omega_t$ and p_{ref} is a reference pressure value at the outlet. Here, Eq. (4a) is the no-slip condition, (4b) is the condition that guarantees that the flow is attached to the airfoil, and (4c) is the so-called do-nothing condition, see [10].

2.2 Airfoil Motion

An airfoil is assumed to be a rigid body with two degrees of freedom (i.e., oscillating both vertically (bending) and angularly (pitching) about the elastic axis EO), see Fig. 1. Under the assumption of small amplitude motion, the governing equations are given by

$$\begin{aligned} m\ddot{h} + k_{hh}h + S_\alpha\ddot{\alpha} + d_{hh}\dot{h} &= -L(t), && \text{(5a)} \\ S_\alpha\ddot{h} + I_\alpha\ddot{\alpha} + k_{\alpha\alpha}\alpha + d_{\alpha\alpha}\dot{\alpha} &= M(t), && \text{(5b)} \end{aligned}$$

where h is the translational displacement (bending), $\dot{h}$ is the translational velocity, $\ddot{h}$ is the translational acceleration, α is the angular displacement (pitching), $\dot{\alpha}$ is the angular velocity, and $\ddot{\alpha}$ is the angular acceleration. In Eq. (5a), m denotes the airfoil's mass, the coefficient k_{hh} represents the stiffness, while S_α is the static moment about the elastic axis EO. The damping coefficient is denoted as d_{hh}, and $L(t)$ represents the external time-dependent lift. Eq. (5b) includes the moment of inertia I_α, the torsional stiffness $k_{\alpha\alpha}$, and structural damping in torsion $d_{\alpha\alpha}$. Lastly, $M(t)$ is the aerodynamic torsional moment, considered positive in the clockwise direction, for a detailed description see [4]. The system (5a-5b) is equipped with the initial conditions that define the values $h(0), \alpha(0), \dot{h}(0), \dot{\alpha}(0)$.

3 Discretization method

Firstly, the problem (2) is semi-discretized in time. The constant time step $\Delta t > 0$ is taken and the time interval $(0, T)$ is equidistantly divided into time intervals (t_n, t_{n+1}) with $t_n = n\Delta t$. Then, the velocity and the pressure at each time step $t_n \in (0, T]$ are approximated as

$$\boldsymbol{u}^n(x) \approx \boldsymbol{u}(x, t_n),\ p^n(x) \approx p(x, t_n), \quad \text{for } x \in \Omega_{t_n}. \tag{6}$$

Similarly, the domain velocity $\boldsymbol{w}$ at time t_{n+1} is approximated as

$$\boldsymbol{w}^{n+1}(x) \approx \boldsymbol{w}(x, t_{n+1}), \quad \text{for } x \in \Omega_{t_{n+1}}. \tag{7}$$

Finally, the ALE derivative is approximated at fixed time step t_{n+1} by the second-order two-step backward difference formula (BDF2), as a result the implicit scheme is obtained in the form

$$\begin{aligned} \frac{3\boldsymbol{u}^{n+1} - 4\tilde{\boldsymbol{u}}^n + \tilde{\boldsymbol{u}}^{n-1}}{2\Delta t} + ((\boldsymbol{u}^{n+1} - \boldsymbol{w}^{n+1}) \cdot \boldsymbol{\nabla})\boldsymbol{u}^{n+1} - \nu \boldsymbol{\Delta} \boldsymbol{u}^{n+1} + \boldsymbol{\nabla} p^{n+1} &= 0, \\ \boldsymbol{\nabla} \cdot \boldsymbol{u}^{n+1} &= 0, \end{aligned}$$

where $\tilde{\boldsymbol{u}}^i$ represents the transformed velocity $\boldsymbol{u}^i$ from Ω_i onto Ω_{n+1}, i.e., $\tilde{\boldsymbol{u}}^i = \boldsymbol{u}^i \circ A_{t_i} \circ A^{-1}_{t_{n+1}}$, see [3].

3.1 Finite element method

The finite element discretization of Problem (8) begins with the so-called weak formulation, which is introduced in the standard way. To this purpose, the simplified notation at the fixed time instant t^{n+1} is used: $\boldsymbol{u} = \boldsymbol{u}^{n+1}$, $\boldsymbol{w} = \boldsymbol{w}^{n+1}$, $p = p^{n+1}$, and $\Omega = \Omega_{t_{n+1}}$. Moreover, the velocity test space $\boldsymbol{\mathcal{V}}$ and the pressure test space $\mathcal{Q}$ are defined as

$$\boldsymbol{\mathcal{V}} = \left\{ \boldsymbol{\varphi} \in \boldsymbol{H}^1(\Omega) : \boldsymbol{\varphi}(x) = 0\ \forall x \in \Gamma_D \cup \Gamma_W \right\}, \quad \mathcal{Q} = L^2(\Omega), \tag{8}$$

where $\boldsymbol{H}^1(\Omega) = [H^1(\Omega)]^2$ denotes the vector Sobolev space and $L^2(\Omega)$ is the Lebesgue space, see [11]. Additionally, the scalar product is denoted by $(\boldsymbol{u}, \boldsymbol{v})_\Omega = \int_\Omega \boldsymbol{u} \cdot \boldsymbol{v}\ \mathrm{d}x$ in $\boldsymbol{L}^2(\Omega)$ and the trilinear form is given by $c(\boldsymbol{u}, \boldsymbol{v}, \boldsymbol{w}) = \int_\Omega [(\boldsymbol{u} \cdot \nabla)\boldsymbol{v}] \cdot \boldsymbol{w}\ \mathrm{d}x$. Additionally, the following forms are introduced

$$\begin{aligned} a\left(U^*, U, V\right) &= \frac{3}{2\Delta t}(\boldsymbol{u}, \boldsymbol{v})_\Omega + \nu(\nabla \boldsymbol{u}, \nabla \boldsymbol{v})_\Omega + c(\boldsymbol{u}^* - \boldsymbol{w}, \boldsymbol{u}, \boldsymbol{v}) - (p, \nabla \cdot \boldsymbol{v})_\Omega - (\nabla \cdot \boldsymbol{u}, q)_\Omega, \\ F\left(V\right) &= \frac{1}{2\Delta t}(4\tilde{\boldsymbol{u}}^n - \tilde{\boldsymbol{u}}^{n-1}, \boldsymbol{v})_\Omega, \end{aligned} \tag{9}$$

where $U^* = (\boldsymbol{u}^*, p^*)$, $U = (\boldsymbol{u}, p)$, and $V = (\boldsymbol{v}, q)$, see [5].

Let us take arbitrary test functions $\mathbf{v} \in \boldsymbol{\mathcal{V}}$ and $q \in \mathcal{Q}$, multiply Eqs. (8). Furthermore, integrate over the domain Ω and by some mathematical operations the weak formulation is gained in the form: Find $U = (\boldsymbol{u}, p) \in \boldsymbol{\mathcal{V}} \times \mathcal{Q}$ which satisfy

$$a\left(U, U, V\right) = F(V), \quad \forall V \in \boldsymbol{\mathcal{V}} \times \mathcal{Q}, \tag{10}$$

and $\boldsymbol{u}$ the conditions (4a-4b). In order to solve nonlinear problem, the so-called Oseen's linearization is used, see [4].

To apply the finite element method (FEM), an admissible triangulation of the domain Ω is assumed, see [12]. On this triangulation, finite element (FE) subspaces are defined, generally consisting of piecewise polynomial functions. The choice of velocity and pressure spaces must satisfy the Babuška-Brezzi inf-sup condition, which is necessary for the stability of the numerical scheme, see [5]. This paper considers two such elements. The first is the so-called Taylor-Hood (TH) element:

$$\boldsymbol{\mathcal{V}}_h = \left\{\boldsymbol{\varphi} \in \mathbf{C}(\overline{\Omega}) : (\boldsymbol{\varphi}\big|_K \in P_2(K), \forall K \in \tau_h)\right\} \cap \boldsymbol{\mathcal{V}}, \tag{11}$$

$$\mathcal{Q}_h = \left\{\varphi \in C(\overline{\Omega}) : (\varphi\big|_K \in P_1(K), \forall K \in \tau_h)\right\}. \tag{12}$$

TH element satisfies the BB condition on a regular triangulation, but the divergence constraint is satisfied only discretely, see [6]. This issue is addressed by using the Scott-Vogelius (SV) element, which is pressure-robust. In this case the velocity space remains defined as in (11), while the pressure space is replaced by discontinuous piecewise linear element:

$$\mathcal{Q}_h^{disc} = \left\{\varphi : \overline{\Omega} \to \mathbb{R} : (\varphi\big|_K \in P_1(K), \forall K \in \tau_h)\right\}. \tag{13}$$

The SV element satisfies the BB condition, provided that a barycentric refinement of a regular triangulation is used. As the pressure is continuous only within each element and the mesh is refined, consequently, computations are significantly more expensive when using the SV element. On the other hand, the divergence constraint is strongly satisfied.

On the FE spaces mentioned above, the discrete problem (10) reads: Find $U_h \in \boldsymbol{\mathcal{V}}_h \times \mathcal{Q}_h$ which satisfy

$$a\left(U_h{}^*, U_h, V_h\right) = f(V_h), \tag{14}$$

for all $V_h \in \boldsymbol{\mathcal{V}}_h \times \mathcal{Q}_h$.

The problem (14) requires stabilization in the considered case of flows with dominated convection, see [13]. The classical streamline upwind Petrov-Galerkin (SUPG) method is used with the TH element, but the SV element is stabilized by using classical streamline diffusion, as it cannot be applied with the SV element due to the coupling of pressure p and velocity $\boldsymbol{u}$, see [14, 15]. Moreover, as the TH element satisfies the divergence constraint only discretely, the grad-div stabilization is employed, see [7, 16].

4 Numerical experiments

In this section, the numerical results of both described methods are compared with the available reference data.

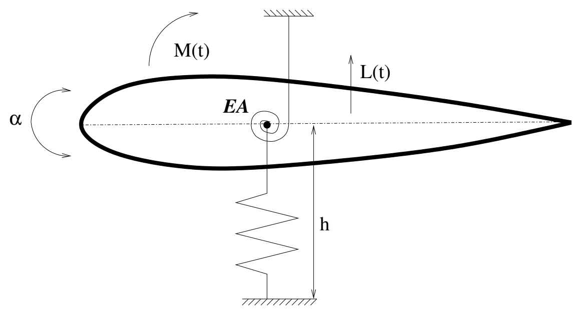

Figure 1: Structural set-up of the NACA0012 airfoil.

The ALE transformation is approximated by using the pseudo-elastic approach, see [3]. For space discretization of the Navier-Stokes equations, the SV and TH elements are considered while the ALE derivative is approximated by the BDF2. The structural motion (5a-5b) are approximated by the 4-th order Runge-Kutta method. A strong coupling algorithm is used, as described in [3].

The test case is the complete fluid-structure interaction problem, where the results obtained by both elements are compared with each other, with the NASTRAN prediction, see [9], and with the aero-elastic theory, see [8]. In this paper a grid with 22571 vertices and 44296 triangular elements was used. The total number of unknowns (degrees of freedom / DOF) was 201447 for the TH element. For the case of the SV element the mesh with 17163 vertices, 33930 elements, and total 231790 DOF was used with the Scott-Vogelius (SV) element. The grid was refined in order to capture the boundary layer around the airfoil and the wake behind it.

The following quantities are considered: $m = 0.086622$ kg, $S_\alpha = 0.000779673$ kg m, $I_\alpha = 0.000487291$ kgm^2, $k_{hh} = 105.109$ N/m, $k_{\alpha\alpha} = 3.695582$Nm/rad, $l = 0.05$ m, $c = 0.3$ m. Here, l is the depth of the airfoil and c is its chord length. The proportional damping coefficients are considered in the form $d_{hh} = \epsilon_f k_{hh}$ and $d_{aa} = \epsilon_f k_{aa}$, where we choose $\epsilon_f = 10^{-3}$. In addition, the fluid properties are $\rho = 1.225$ kg/m^3, $\nu = 1.5 \times 10^{-5}$ m/s^2.

The far-field velocity (U_{ref}) is varied to examine the structural response to a given initial displacement. The values of U_{ref} considered are $U_{\mathrm{ref}} \in [2, 35]$, which yields the Reynolds number $\mathrm{Re} = \frac{U_{\mathrm{ref}} c}{\nu}$ in the range 4×10^4 to 7×10^5. The structure's initial conditions are specified as follows

$$h(0) = h_0 = 20\,\mathrm{mm}, \quad \dot{h}(0) = 0, \quad \alpha(0) = \alpha_0 = 6^\circ, \quad \dot{\alpha}(0) = 0.$$

In Figs. 2, the flow field is presented for $U_{\mathrm{ref}} = 8\,\mathrm{m/s}$. It can be seen that the initial displacement is stabilized and that there is no aerodynamic amplification, see Figs. 3, where the bending and pitching displacements as a function of time are shown. The results indicate that for $U_{\mathrm{ref}} = 8\,\mathrm{m/s}$, the flow stabilizes the displacements. However, for values $U_{\mathrm{ref}} = 32\,\mathrm{m/s}$, the initial displacement is amplified, leading to a vibration resembling the limit cycle of the oscillations, see Fig. 4. This corresponds to the results presented in [9], where the critical speed is $U_{crit} = 30.25\,\mathrm{m/s}$.

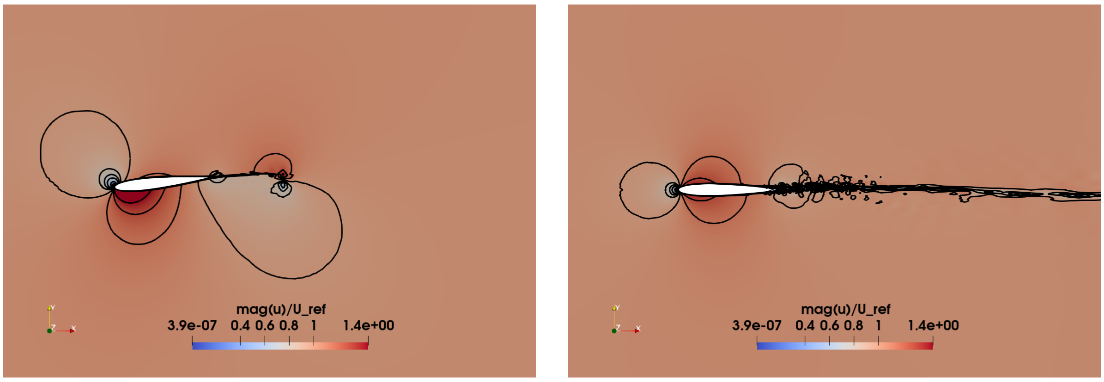

a) b)

Figure 2: The magnitudes of the velocity $||\boldsymbol{u}||_\infty$ for the $U_{\mathrm{ref}} = 8$ obtained by the TH element: a) $t = 0$ and b) $t = 1.5$.

In Figs. 5, the dominant frequencies are presented obtained by the Theodorsen theory and FE approximations, see [8]. Both elements agree with aerodynamic theory. However, the SV element agrees only up to $U_{\mathrm{ref}} = 20\,\mathrm{m/s}$, as the stream-line diffusion is used for stabilization, which reduces the order of the method. To solve the problem of reduced order, mesh refinement would typically be applied. However, this is not possible due to the limitations of the UMFPACK library as the solver, see [17]. Furthermore, it can be observed that as U_{ref} increases, the dominant frequencies approach each other until resonance is reached.

Finally, the damping coefficients are given in Figs. 6. As the far-field velocity increases, the damping effect increases to $25\,\mathrm{m/s}$. However, beyond this point, further increases in velocity reduce the damping ratio for both pitching and bending. Above $30\,\mathrm{m/s}$, the damping ratio of pitching is positive, leading to a flutter-type instability. These results align with those obtained using NASTRAN, which predicts critical flow speeds of $U_{\mathrm{ref}} = 30.25\,\mathrm{m/s}$ for pitching (flutter), as noted in [9].

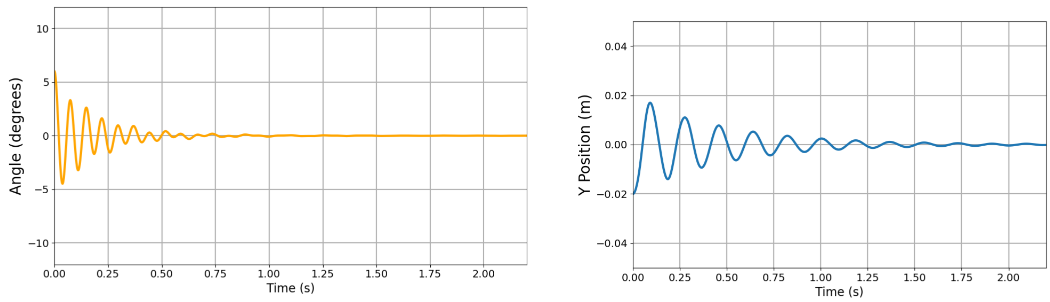

a) b)

Figure 3: Bending a) and pitching b) for the $U_{\mathrm{ref}} = 8\,\mathrm{m/s}$ with using the TH element.

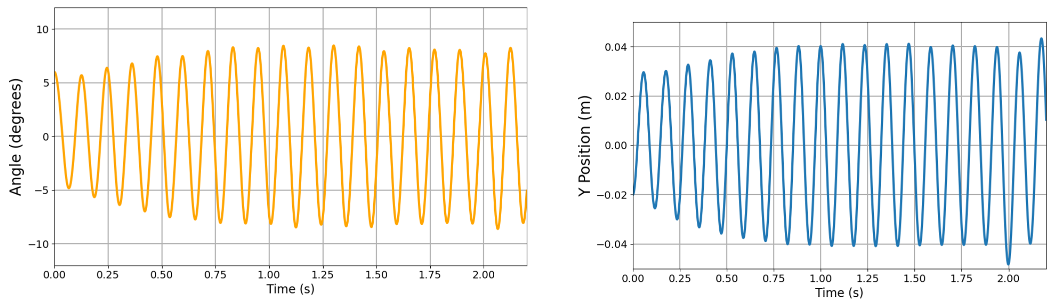

c) d)

Figure 4: Bending a) and pitching b) for the $U_{\mathrm{ref}} = 32\,\mathrm{m/s}$ with using the TH element.

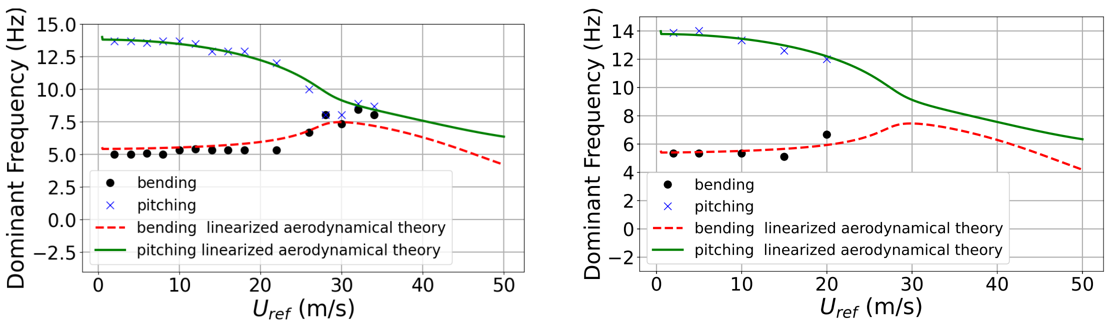

a) b)

Figure 5: Comparison of dominant frequencies obtained by the TH element a) SV element b) with the results from [8].

5 Conclusion

This paper presents a numerical study of a complete fluid-structure interaction (FSI) problem involving a fluid flow around the airfoil with two degrees of freedom. The governing equations consist of the incompressible Navier-Stokes equations formulated in the Arbitrary Lagrangian-Eulerian (ALE) framework for the fluid due to the moving domain, and a system of ordinary differential equations describing the airfoil's motion with two degrees of freedom: bending and pitching. The numerical solution is obtained using the in-house solver which is based on the finite element method (FEM). Two discretizations are considered which satisfy the Babuška-Brezzi (BB) condition: Taylor-Hood (TH) and Scott-Vogelius (SV). Stabilization techniques, including the streamline upwind Petrov-Galerkin (SUPG) method and grad-div stabilization, are applied to

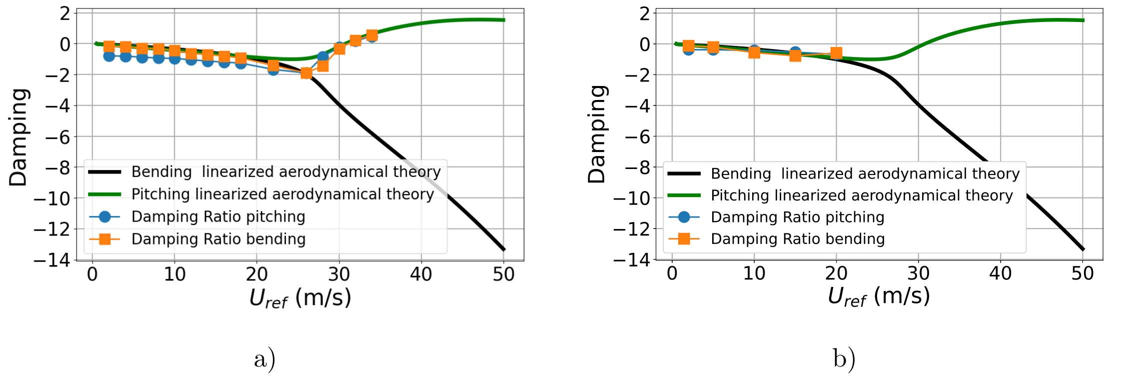

Figure 6: Comparison of damping obtained by the TH element a) SV element b) with the results from [8].

address convection dominance. The TH element achieves stability through SUPG and grad-div techniques, while the SV element uses streamline diffusion for stabilization (it is not possible to use SUPG with the SV element due to the strong coupling between the velocity and the pressure).

The numerical models were tested on the reference problem of the flow around the NACA0012 with two degrees of freedom. The far-field velocity U_{ref} varies, and the response to the initial displacement was evaluated. The dominant frequencies for bending and pitching were compared with the data obtained by the matlab script based on the classical aero elastic theory [8] and the critical velocity was compared with the predictions of NASTRAN [9]. The results show that for $U_{\mathrm{ref}} \leq 20$, both elements are in excellent agreement with the theory. However, for higher velocities, the results could not be obtained with the SV element, as the streamline diffusion stabilization reduces the method's order, whereas the TH element shows agreement for all cases.

The study further shows that as the far-field velocity increases, the damping effect initially increases but decreases beyond $U_{\mathrm{ref}} = 25\,\mathrm{m/s}$. At $U_{\mathrm{ref}} = 32\,\mathrm{m/s}$, a flutter-type instability occurs. These observations are in agreement with [9], where the critical flow speed is $U_{\mathrm{ref}} = 30.25\,\mathrm{m/s}$.

In conclusion, the Taylor-Hood and Scott-Vogelius elements provide reliable results within their respective stability ranges. The numerical results are in strong agreement with theoretical benchmarks, confirming the robustness and accuracy of the presented methods. The only disadvantage is in the stabilization of the SV element. This might be future work to use some advanced approach for stabilization such as local projection method or variational multi scale method, see [18, 1].

Acknowledgment

This work was supported by the Czech Technical University in Prague under the grant No. *Grant SGS22/148/OHK2/3T/12* and the grant No. *Grant SGS24/120/OHK2/3T/12*. Karel Vacek has been supported by the Czech Science Foundation (GAČR) project 22-01591S. The Institute of Mathematics, CAS is supported by RVO:67985840. The authors gratefully acknowledge the Center of Advanced Aerospace Technology (CZ.02.1.01/0.0/0.0/16_019/0000826) at the Czech Technical University in Prague for awarding access to computing facilities.

References

[1] Sváček, P.: On numerical simulation of fluid-structure interaction problems using variational multiscale methods. *Journal of Computational and Applied Mathematics*, vol. 427, (2023), pp. 115–125.

[2] Takashi, N. & Hughes, T. J. R.: An arbitrary Lagrangian-Eulerian finite element method for interaction of fluid and a rigid body. *Computer Methods in Applied Mechanics and Engineering*, vol. 95, no. 1, (1992), pp. 115–138.

[3] Feistauer, M., Horacek, J., Ruzika, M. & Svacek, P.: Numerical analysis of flow-induced nonlinear vibrations of an airfoil with three degrees of freedom. *Computers & Fluids*, vol. 49, no. 1, (2011), pp. 110–127.

[4] Sváček, P., Feistauer, M. & Horáček, J.: Numerical simulation of flow induced airfoil vibrations with large amplitudes. *Journal of Fluids and Structures*, vol. 23, no. 3, (2007), pp. 391–411.

[5] Girault, V. & Raviart, P.A.: Finite Element Methods for Navier-Stokes Equations: Theory and Algorithms. *Computational Mathematics Series*, (1986).

[6] Case, M. A., Ervin, V. J., Linke, A. & Rebholz, L. G.: A connection between Scott—Vogelius and grad-div stabilized Taylor—Hood FE approximations of the Navier—Stokes equations. *SIAM Journal on Numerical Analysis*, vol. 49, (2011), pp. 1461–1481.

[7] Jenkins, E. W., John, V., Linke, A. & Rebholz, L. G.: On the parameter choice in grad-div stabilization for the Stokes equations. *Advances in Computational Mathematics*, vol. 40, (2014), pp. 491–516.

[8] Theodorsen, T.: General theory of aerodynamic instability and the mechanism of flutter. *NASA reference publication*, (1934).

[9] Cecrdle, J. & Malecek, J.: Verification FEM model of an aircraft construction with two and three degrees of freedom. *Technical Report Research Report R-3418/02, Aeronautical Research and Test*, (2002).

[10] Turek, S.: Efficient solvers for incompressible flow problems: An algorithmic and computational approach. *Springer Science & Business Media*, vol. 6, (1999).

[11] Kufner, A., John, O. & Fucik, S.: Function Spaces. (1977).

[12] Ciarlet, P. G.: The Finite Element Method for Elliptic Problems. (2002).

[13] John, V. & Schmeyer, E.: Finite element methods for time-dependent convection-diffusion-reaction equations with small diffusion. *Computer Methods in Applied Mechanics and Engineering*, vol. 198, no. 3-4, (2008), pp. 475–494.

[14] Ahmed, N., Barrenechea, G. R., Burman, E., Guzmán, J., Linke, A. & Merdon, C.: A pressure-robust discretization of Oseen's equation using stabilization in the vorticity equation. *SIAM Journal on Numerical Analysis*, vol. 59, no. 5, (2021), pp. 2746–2774.

[15] Beirão da Veiga, L., Dassi, F. & Vacca, G.: Pressure robust SUPG-stabilized finite elements for the unsteady Navier-Stokes equation. *IMA Journal of Numerical Analysis*, (2023).

[16] Olshanskii, M. & Reusken, A.: Grad-div stabilization for Stokes equations. *Mathematics of Computation*, vol. 73, no. 248, (2004), pp. 1699–1718.

[17] Raju, M. & Khaitan, S. K.: High Performance Computing of Three-Dimensional Finite Element Codes on a 64-bit Machine. *Journal of Applied Fluid Mechanics*, vol. 5, (2012).

[18] Burman, E. & Linke, A.: Stabilized finite element schemes for incompressible flow using Scott–Vogelius elements. *Applied Numerical Mathematics*, vol. 58, no. 11, (2008), pp. 1704–1719.